Simvastatin-Romidepsin Combination Kills Bladder Cancer Cells Synergistically

Kazuki Okubo
National Defense Medical College
Kosuke Miyai
National Defense Medical College
Kimi Kato
National Defense Medical College
Takako Asano
National Defense Medical College
Akinori Sato (zenpaku@ndmc.ac.jp)
National Defense Medical College https://orcid.org/0000-0001-9011-1756

Research

Keywords: bladder cancer, metastatic, apoptosis, AMPK

Posted Date: July 2nd, 2020

DOI: https://doi.org/10.21203/rs.3.rs-38694/v1

Version of Record: A version of this preprint was published at Translational Oncology on September 1st, 2021. See the published version at https://doi.org/10.1016/j.tranon.2021.101154.

Abstract

Background

The HMG-CoA reductase inhibitor simvastatin activates AMP-activated protein kinase (AMPK) and thereby induces histone acetylation. We postulated that combining simvastatin with the histone deacetylase (HDAC) inhibitor romidepsin would kill bladder cancer cells by inducing histone acetylation cooperatively.

Methods

Bladder cancer cells (UMUC-3, T-24, J-82, MBT-2) were treated with simvastatin and romidepsin. Cell viability and clonogenicity were assessed by CCK-8 assay and colony formation assay. *In-vivo* efficacy was evaluated using murine subcutaneous tumor models. Flow cytometry was used to detect annexin-V positive cells and to evaluate cell cycle distribution and cellular reactive oxygen species (ROS) production. Induction of histone acetylation and the expression of AMPK, HDACs, peroxisome proliferator-activated receptor (PPAR) γ, cell-cycle regulators, and the endoplasmic reticulum (ER) stress markers were evaluated by western blotting.

Results

The combination of romidepsin and simvastatin induced robust apoptosis and killed bladder cancer cells synergistically (combination indexes < 1). It also suppressed colony formation significantly. In murine subcutaneous tumor models using MBT-2 cells, a 15-day treatment with 0.5 mg/kg romidepsin and 15 mg/kg simvastatin was well tolerated and inhibited tumor growth significantly. Mechanistically, the combination induced histone acetylation by activating AMPK. The combination also decreased the expression of HDACs, thus further promoting histone acetylation. This AMPK activation was essential for the combination's action because compound C, an AMPK inhibitor, suppressed the combination-induced histone acetylation and the combination's ability to induce apoptosis. We also found that the combination increased the expression of PPARγ, leading to ROS production. Furthermore, the combination induced ER stress and this ER stress was shown to be associated with increased AMPK expression and histone acetylation, thus playing an important role in the combination's action. Our study also suggests there is a positive feedback cycle between ER stress induction and PPARγ expression.

Conclusions

The combination of simvastatin and romidepsin kills bladder cancer cells synergistically. Its mechanism of action includes ER stress induction, AMPK activation, histone acetylation, and increased PPARγ expression.

Background

There is currently no curative treatment for metastatic bladder cancer and development of novel treatment strategy is urgently needed. AMP-activated protein kinase (AMPK) is a cellular energy sensor, which is activated by impaired energy status such as glucose deprivation, ischemia, hypoxia, and oxidative stress, leading to inhibition of cellular growth to restore energy homeostasis [1]. Therefore, drugs activating AMPK have attracted much attention as novel anticancer agents [2–5]. HMG-CoA reductase inhibitors, which are widely used for treating dyslipidemia [6–9], are known to activate AMPK [10–12]. Simvastatin inhibits HMG-CoA reductase and has been shown to kill cancer cells in vitro [12–14], although its anticancer efficacy has not been proven yet in clinical trials [15].

Background

There is currently no curative treatment for metastatic bladder cancer and development of novel treatment strategy is urgently needed. AMP-activated protein kinase (AMPK) is a cellular energy sensor, which is activated by impaired energy status such as glucose deprivation, ischemia, hypoxia, and oxidative stress, leading to inhibition of cellular growth to restore energy homeostasis [1]. Therefore, drugs activating AMPK have attracted much attention as novel anticancer agents [2–5]. HMG-CoA reductase inhibitors, which are widely used for treating dyslipidemia [6–9], are known to activate AMPK [10–12]. Simvastatin inhibits HMG-CoA reductase and has been shown to kill cancer cells in vitro [12–14], although its anticancer efficacy has not been proven yet in clinical trials [15].

Histone acetylation is an innovative epigenetics-based cancer therapy [16, 17] and preclinical studies showed that histone deacetylase (HDAC) inhibitors were capable of inhibiting bladder cancer growth [18–20]. Romidepsin is a class I HDAC inhibitor clinically approved for the treatment of cutaneous T cell lymphoma [21–23], which acts against cancer cells at lower concentrations in vitro, but the clinical benefit against solid tumors is not satisfactory [24–26].

Recently, AMPK activation has been shown to induce histone acetylation [27, 28]. We thought that simvastatin would activate AMPK and the simvastatin-romidepsin combination would kill bladder cancer cells effectively by inducing histone cooperatively. We also investigated the role of endoplasmic reticulum (ER) stress induction in the combination's anticancer activity because histone acetylation is closely related to ER stress induction [29, 30]. Furthermore, simvastatin is known to activate peroxisome proliferator-activated receptor (PPAR) γ, a regulator of fatty acid storage and glucose metabolism [31–33], which plays a crucial role in bladder cancer proliferation [34–36]. Therefore, we also evaluated the contribution of PPARγ activation to the anticancer activity of the simvastatin-romidepsin combination and its association with histone acetylation and ER stress induction.

Methods

Cell culture

Human bladder cancer cells (UMUC-3, T-24, and J-82) were purchased from the American Type Culture Collection (Rockville, MD, USA) and murine bladder cancer cells (MBT-2) were purchased from Japanese Collection of Research Bioresources Cell Bank (Osaka, Japan). The cells were cultured in the recommended media (minimum essential medium and McCoy's 5A medium) supplemented with 10% fetal bovine serum and 1.0% penicillin/streptomycin (Invitrogen, Carlsbad, CA, USA) at 37°C under 5% CO_2 in a humidified incubator.

Reagents

Simvastatin and vorinostat purchased from Cayman Chemical (Ann Arbor, MI, USA), romidepsin, belinostat and entinostat purchased from Selleck Chemicals (Houston, TX, USA), panobinostat purchased from LC Laboratories (Boston, MA, USA), and rosiglitazone and tunicamycin purchased from Enzo Life Sciences (Farmingdale, NY, USA) were dissolved in dimethyl sulfoxide (DMSO). Compound C dihydrochloride purchased from R&D Systems (Minneapolis, MN, USA) and cycloheximide purchased from Enzo Life Sciences were dissolved in distilled water. These reagents were stored at −80°C or −20°C until use.

Cell viability assay

5×10^3 cells were seeded into each well of a 96-well culture plate one day before being treated with the indicated conditions. After treatment, cell viability was evaluated by CCK-8 assay (Dojindo, Kumamoto, Japan) according to the manufacturer's protocol.

Cell confluency assay

5×10^3 cells were seeded into each well of a 96-well culture plate one day before being treated with indicated conditions. After treatment, confluence measurements were performed at 3-hour intervals over 3 days by the IncuCyte real-time video imaging system (Essen Instruments, Ann Arbor, MI, USA).

Clonogenic assay

2 or 3×10^2 cells (the number depended on the cell line) were seeded into each well of a 12-well culture plate one day before being treated for 48 hours with 5 μM simvastatin and/or 20 nM romidepsin. The cells were then given fresh medium and cultured for 1 to 2 weeks. The colonies were counted after being fixed with 100% methanol and stained with Giemsa's solution.

In-vivo study

The *in-vivo* efficacy of the simvastatin-romidepsin combination was assessed using murine subcutaneous allograft models. Animal studies were conducted in compliance with Japanese animal use regulations and approval for these studies was obtained from the institutional Animal Care and Use Committee of National Defense Medical College. 1×10^7 MBT-2 cells were implanted subcutaneously into C3H/HeN Slc mice purchased from Japan SLC (Shizuoka, Japan) and treatment was initiated five days

later (day 1), when all the mice exhibited measurable tumors. The mice were divided into the vehicle group and the treatment groups (n = 5 per group). The vehicle group received intraperitoneal injections of DMSO, and the treatment groups received 0.5 mg/kg romidepsin or 15 mg/kg simvastatin or both. The injections of romidepsin were given twice per week and the injections of simvastatin were given once a day for 15 days (5 days on 2 days off). Tumor volume and body weight were measured every 2 or 3 days. Tumor volumes were estimated using the following formula: volume = 0.5 × length × width^2. After 15 days of treatment, the animals were euthanized in compliance with the United Kingdom National Cancer Research Institute's ethical policy [37] and the subcutaneous tumors were harvested.

Flow cytometry

Flow cytometry was used for analysis of annexin-V assay and cell cycle and evaluation of cellular reactive oxygen species (ROS) production. Briefly, 1.0 × 10^5 cells were seeded into each well of a 12-well culture plate one day before being cultured for 48 hours under the indicated conditions. Cells were then washed with phosphate-buffered saline and harvested by trypsinization. For annexin-V assay, cells were subjected to annexin V and 7-amino-actinomycin D (7-AAD) double staining following the protocol of the assay kit's manufacturer (Beckman Coulter, Marseille, France). For cell cycle analysis, cells were resuspended in citrate buffer and stained with propidium iodide. For evaluation of cellular ROS production, cells were stained with dihydroethidium (DHE) (Cayman Chemical) according to the manufacturer's protocol. The cells were then analyzed using a flow cytometer and CellQuest Pro Software (BD Biosciences, San Jose, CA, USA). Three independent tests were performed.

Western blotting

After treating bladder cancer cells under the indicated conditions for 48 hours, whole cell lysates were obtained using radioimmunoprecipitation assay buffer. Equal amounts of protein were separated by sodium dodecyl sulfate-polyacrylamide gel electrophoresis and transferred to nitrocellulose membranes. After the membranes were blocked with 5% skimmed milk, they were incubated with the primary antibodies: anti-AMPK and anti-PPARγ from Proteintech (Rosemont, IL, USA); anti-phosphorylated AMPK (p-AMPK), anti-phosphorylated histone H2AX (p-H2AX), and anti-endoplasmic reticulum resident protein (ERp) 44 from Cell Signaling Technology (Danvers, MA, USA); anti-glucose-regulated protein (GRP) 78, anti-cyclin D1, anti-cyclin E, anti-cyclin-dependent kinase (CDK) 2, anti-CDK4, anti-HDAC1, anti-HDAC3, and anti-HDAC6 from Santa Cruz Biotechnology (Santa Cruz, CA, USA); anti-acetylated histone from Abcam (Cambridge, UK); and anti-actin from Millipore (Billerica, MA, USA). Then the protein was detected by reaction with recommended secondary antibody (horseradish-tagged goat anti-rabbit or goat anti-mouse antibody (GE Healthcare UK, Amersham, UK)) and staining with chemiluminescence solution (Clarity Western ECL Substrate, Bio-Rad, Hercules, CA, USA) and imaged with ChemiDoc Touch Imaging System (Bio-Rad).

Statistical analysis

CalcuSyn software (Biosoft, Cambridge, UK) was used for calculating the combination indexes according to the method developed by Chou and Talalay [38]. The statistical significance of observed differences between samples was evaluated using the Mann-Whitney U test (JMP Pro14 software, SAS Institute, Cary, NC, USA), and differences for which $p < 0.05$ were considered statistically significant.

Results

Anticancer activity of simvastatin and romidepsin in bladder cancer cells

Simvastatin inhibited the growth of bladder cancer cells in a dose- and time-dependent manner (Fig. 1a and b). Mechanistically, it increased both the phosphorylation and expression of AMPK, thus activating AMPK, and induced histone acetylation (Fig. 1c). Furthermore, simvastatin induced ER stress evidenced by the increased expression of GRP78 and ERp44 (Fig. 1c). We also found that simvastatin increased the expression of PPARγ (Fig. 1c), a transcriptional regulator of glucose and lipid metabolism [31–33]. Interestingly, The Cancer Genome Atlas data analysis by using the UCSC Cancer Browser UCSC Xena (https://xena.ucsc.edu/welcome-to-ucsc-xena/) revealed that bladder cancer patients with higher expression of PPARγ genes had longer overall survival time than those with lower expression (Additional file 1: Fig. S1).

We then tested the antiproliferative activity of various HDAC inhibitors in bladder cancer cells and found that romidepsin had the lowest IC50 value among them (Fig. 1d and Table 1). We therefore used romidepsin in the subsequent experiments. Romidepsin inhibited bladder cancer proliferation in a dose- and time-dependent manner (Fig. 1e and f). Mechanistically, it induced not only histone acetylation but also ER stress (Fig. 1g).

Anticancer activity of the simvastatin-romidepsin combination in bladder cancer cells

A 48-hour treatment with the combination of simvastatin and romidepsin inhibited bladder cancer growth effectively (Fig. 2a and b), and the synergism of the combination's effect was confirmed in all the treatment conditions (Table 2 and Additional file 2: Fig. S2). We also found that the combination's antiproliferative effect was time-dependent (Fig. 2c and Additional file 3: Video images 1). Furthermore, the combination inhibited the clonogenic survival of bladder cancer cells significantly (Fig. 2d). Thus, the combination of simvastatin and romidepsin was shown to inhibit bladder cancer growth effectively.

We then evaluated changes in the cell cycle and apoptosis caused by the combination of simvastatin and romidepsin. The combination perturbed the cell cycle and significantly increased the number of the cells in the sub-G1 fraction (Fig. 2e), suggesting that it caused DNA fragmentation and induced apoptosis. The increased expression of p-H2AX proved that the combination caused DNA double strand breaks (Fig. 2f). The combination decreased the expression of the cell cycle regulators, cyclin D1, cyclin E, CDK2, and CDK4 (Fig. 2f), which was consistent with the perturbation of the cell cycle. Furthermore, the combination significantly increased the percentage of the cell population that was annexin-V positive (Fig. 2g), confirming that the combination induced apoptosis cooperatively.

In consistence with our hypothesis, simvastatin enhanced romidepsin-induced histone acetylation (Fig. 2h). Simvastatin activated AMPK and, interestingly, this activation was further promoted by romidepsin (Fig. 2h). Our previous studies showed that ER stress activates AMPK [29, 30], so we thought that the combination of romidepsin and simvastatin would also induce ER stress and thereby enhance AMPK activation. As expected, the combination induced ER stress cooperatively (Fig. 2i). We also found that the combination decreased the expression of HDAC1, 3, and 6 (Fig. 2i), which might further enhance the histone acetylation and ER stress. Furthermore, the simvastatin-romidepsin combination increased the expression of PPARγ cooperatively (Fig. 2h), which was consistent with the combination-increased ROS production (Fig. 2j) because PPARγ activation triggers a metabolic switch that inhibits pyruvate oxidation resulting in an increase of cellular ROS levels [39].

AMPK activation was responsible for the enhanced histone acetylation and cytotoxicity caused by the simvastatin-romidepsin combination

We then investigated the role of AMPK activation in the combination's action. The cells were treated with the simvastatin-romidepsin combination with or without the AMPK inhibitor compound C. Compound C significantly decreased the combination-induced increase of annexin-V positive cells, showing that inhibition of AMPK attenuated the combination-induced apoptosis (Fig. 3a). Furthermore, compound C suppressed the combination-enhanced histone acetylation (Fig. 3b). Thus, the AMPK activation was shown to be responsible for the enhanced histone acetylation and cytotoxicity caused by the combination.

PPARγ activation played a pivotal role in killing bladder cancer cells

Romidepsin and simvastatin increased the expression of PPARγ cooperatively (Fig. 2h). To further investigate the role of PPARγ activation in killing bladder cancer cells, we treated the cells with the PPARγ activator rosiglitazone. Rosiglitazone inhibited the proliferation of bladder cancer cells in a dose-dependent manner (Fig. 4a), showing that PPARγ activation actually had an antiproliferative effect in bladder cancer cells. Although rosiglitazone is essentially a PPARγ agonist, not a transcription activator, it increased the expression of PPARγ in T24 cells (Fig. 4b). Interestingly, rosiglitazone also induced ER stress and histone acetylation in a dose-dependent manner (Fig. 4b), suggesting that PPARγ activation regulates ER stress and histone acetylation.

We then treated the cells with rosiglitazone in combination with romidepsin to investigate romidepsin's ability to enhance PPARγ activator activity. The rosiglitazone-romidepsin combination inhibited the growth of bladder cancer cells synergistically (Fig. 4c, Table 3, and Additional file 4: Fig. S3). It also cooperatively increased ROS production (Fig. 4d) and induced apoptosis (Fig. 4e). Mechanistically, the combination induced ER stress and histone acetylation cooperatively (Fig. 4f). These results suggested that PPARγ activation and consequent ER stress induction and histone acetylation played a pivotal role in killing bladder cancer cells exposed to the simvastatin-romidepsin combination.

ER stress induction is also an important mechanism of the combination's action

We next evaluated the contribution of ER stress induction to the combination's action. Cycloheximide (CHX) is a protein synthesis inhibitor and a suppressor of ER stress induction [40], so we evaluated whether it attenuated the combination's antineoplastic activity. CHX significantly decreased the combination-induced increase in the number of the annexin-V positive cells (Fig. 5a), showing that ER stress induction also played an important role in the combination's antineoplastic effect. Mechanistically, CHX inhibited the combination-induced ER stress and histone acetylation (Fig. 5b), confirming that the histone acetylation was a consequence of the ER stress induction. Unexpectedly, CHX also inhibited the combination-increased PPARγ expression (Fig. 5b) and ROS production (Fig. 5c), suggesting that ER stress induction also regulates the PPARγ expression. To confirm the mechanism that ER stress induction kills bladder cancer cells, we then treated the cells with the ER stress inducer tunicamycin [41]. Tunicamycin inhibited the viability of bladder cancer cells in a dose-dependent manner (Fig. 5d) and increased the expression of AMPK, acetylated histone, and PPARγ (Fig. 5e). Thus, ER stress induction was also shown to be an important mechanism of the combination's action, regulating the expression of AMPK, acetylated histone, and even PPARγ.

The simvastatin-romidepsin combination inhibited bladder cancer growth *in vivo*

Finally, the *in-vivo* anticancer activity of the simvastatin-romidepsin combination was evaluated using mice MBT-2 allograft models. A 15-day treatment with the combination of simvastatin and romidepsin inhibited tumor growth significantly (Fig. 6a and 6b). Notably, it did not cause loss of body weight (Fig. 6c). Hematoxylin-eosin (HE) staining of the *in-vivo* tumor specimens showed that the combination caused marked tumor necrosis (Fig. 6d). We then analyzed the tumor specimens by western blotting and found that the combination of simvastatin and romidepsin increased the phosphorylation of AMPK and the expression of AMPK, acetylated histone, GRP78, and PPARγ (Fig. 6e), confirming that the combination has the same mechanism of action *in vivo* that it does *in vitro*.

Discussion

Drug repositioning is a novel attractive strategy used for finding new anticancer agents because it could lower the cost of developing new drugs and introduce them into the market quickly [42, 43]. This strategy has also been applied to find therapeutic agents against coronavirus disease 2019 in the midst of a global emergency when there is no time to conduct phase-III trials [44]. Because HMG-CoA reductase inhibitors have various physiological properties such as regulating metabolisms [45, 46], inhibiting inflammation [47, 48], modulating the immune system [49], and inhibiting cancer growth [12–14, 50, 51], they are one of the most potent candidate drugs to be used for purposes other than currently approved ones. Furthermore, they have been reported to act against cancer in an additive or synergistic way when combined with other anticancer agents [52–55]. Simvastatin is a clinically available HMG-CoA reductase inhibitor [56]. Preclinical studies demonstrated that it induces apoptosis and inhibits tumor growth in a variety of cancer cells [12–14, 57, 58]. Combinations of simvastatin and an anticancer agent or radiotherapy have not been effective in patients with advanced cancer (Table 4) [59–64]; however, given

simvastatin's wide-ranging physiological properties, there is still a need to evaluate the anticancer effect of simvastatin in combination with other types of anticancer agents.

AMPK is a molecule which controls cellular energy homeostasis and metabolism essential for cancer proliferation [65, 66] and therefore its activation is considered to be a novel anticancer mechanism [2–5]. Several studies demonstrated that simvastatin inhibits tumor growth by activating AMPK [12–14], and AMPK activation has been shown to induce histone acetylation [27–30]. We therefore thought that combining simvastatin with an HDAC inhibitor would kill cancer cells effectively by inducing histone acetylation cooperatively.

HDAC inhibitors have emerged as innovative anticancer drugs because they can influence chromatin structure by acetylating histone, leading to gene upregulation inducing apoptosis and inhibiting cell proliferation [67–69]. In addition, they are known to increase the amount of unfolded proteins by suppressing the molecular chaperone function, thereby inducing ER stress and killing cancer cells [70–72]. In the present study, we tested several HDAC inhibitors for their antiproliferative effect in bladder cancer cells and found that romidepsin had the lowest IC50 value.

Simvastatin enhanced romidepsin-induced histone acetylation and effectively inhibited the growth of bladder cancer cells. In consistence with our hypothesis, AMPK activation was shown to be responsible for the enhanced histone acetylation and cytotoxicity caused by the combination. Unexpectedly, the simvastatin-induced AMPK activation was further promoted by romidepsin, which might also play a role in enhancing the histone acetylation. This AMPK activation was thought to be due to ER stress induction by the combination because the ER stressor tunicamycin increased the expression of AMPK, which is consistent with the previous reports [29, 30, 73, 74]. ER stress is caused by the accumulation and aggregation of unfolded proteins [75], and excessive ER stress causes apoptosis and kills cancer cells [76–78]. We have demonstrated that ER stress-inducing drugs or drug combinations killed urological cancers effectively [73, 74, 79, 80] and, in fact, tunicamycin actually inhibited bladder cancer growth in a dose-dependent fashion. In the present study, inhibition of ER stress by cycloheximide markedly impaired the combination's ability to cause histone acetylation and induce apoptosis, suggesting that the ER stress induction played a pivotal role in the combination's action. This ER stress-histone acetylation sequence is also consistent with our previous results that there is a crosstalk between histone acetylation and ER stress induction [29, 30, 73, 74, 80]. The decreased expression of HDACs is thought to be a consequence of the ER stress induction according to the previous studies [29, 30, 73, 74, 80]. This HDAC suppression might further enhance the histone acetylation and even the ER stress because HDAC suppression abrogates molecular chaperone function, causing the accumulation of unfolded proteins [70–72]. Thus, the combination forms a vicious cycle of ER stress induction and histone acetylation, killing cancer cells effectively.

In the present study, the combination of simvastatin and romidepsin increased the expression of PPARγ cooperatively. PPAR is a member of a superfamily of nuclear hormone receptors and regulates lipid metabolism as a lipid sensor [81]. Interestingly, activation of PPARγ has been shown to exert both anti-

inflammatory and antineoplastic effects [31–33, 39, 82, 83] and the efficacy of PPARγ agonists has been evaluated in preclinical studies and clinical trials in various cancer patients [84–90]. Also in the present study, the PPARγ agonist rosiglitazone actually inhibited bladder cancer growth. Furthermore, the bladder cancer patients with higher expression of PPARγ genes had longer overall survival time than those with lower expression (Additional file 1: Figure S1). Thus, activation of PPARγ would be an attractive approach to killing bladder cancer cells. HDAC inhibitors were reported to interact cooperatively with PPARγ agonists to kill cancer cells [91–93], and romidepsin actually enhanced the activity of rosiglitazone in the present study. Therefore, we inferred that romidepsin enhanced the ability of simvastatin to increase the expression of PPARγ. ER stress and histone acetylation caused by the combination of simvastatin and romidepsin was thought to be a consequence of the increased PPARγ expression because rosiglitazone itself also induced both ER stress and histone acetylation. On the other hand, inhibition of the combination-caused ER stress decreased the combination-increased PPARγ expression and ER stress induction by tunicamycin increased the PPARγ expression. These results suggest that there is a positive feedback cycle between ER stress induction and PPARγ expression. To our knowledge, this is the first study to show a dual regulation of ER stress induction and PPARγ expression. The possible mechanism of the combination's action is summarized in Fig. S4 (Additional file 5).

Conclusions

The combination of simvastatin and romidepsin kills bladder cancer cells synergistically. The combination's mechanism of action includes ER stress induction, AMPK activation, histone acetylation, and increased PPARγ expression. Our study suggests there is a positive feedback cycle between ER stress induction and the increased PPARγ expression. The present study provides a basis for testing the clinical efficacy of this combination in patients with advanced bladder cancer in the context of drug repositioning.

Abbreviations

7-AAD: 7-amino-actinomycin D

AMPK: AMP-activated protein kinase

CDK: cyclin-dependent kinase

CHX: cycloheximide

CI: combination index

DHE: dihydroethidium

DMSO: dimethyl sulfoxide

ER: endoplasmic reticulum

ERp: endoplasmic reticulum resident protein

FITC: fluorescein isothiocyanate

GRP: glucose-regulated protein

HDAC: histone deacetylase

HE: hematoxylin-eosin

p-AMPK: phosphorylated AMP-activated protein kinase

p-H2AX: phosphorylated histone H2AX

PPAR: peroxisome proliferator-activated receptor

ROS: reactive oxygen species

Declarations

Ethics approval and consent to participate

This study was performed with approval from the institutional Animal Care and Use Committee of National Defense Medical College. All animal experiments complied with the national guidelines for the care and use of laboratory animals.

Consent for publication

Not applicable

Availability of data and materials

All data during this study are included within this published article and additional files. Any material described in the article can be requested directly from corresponding author on reasonable request.

Competing interests

The authors declare that they have no competing interests.

Funding

This work was supported by JSPS KAKENHI Grant Number JP18K09183.

Authors' contributions

KO and AS designed the study. KO carried out all the experiments. TA contributed to data collection and animal preparation. KM and KK helped perform immunohistochemistry. KO, KM, KK, TA, and AS

contributed to the interpretation of the results. KO wrote the manuscript with input from all authors. AS supervised the study and edited the manuscript. All authors read and approved the final manuscript.

Acknowledgements

None

References

1. Mihaylova MM, Shaw RJ. The AMPK signalling pathway coordinates cell growth, autophagy and metabolism. Nat Cell Biol. 2011;13:1016-23.
2. Faubert B, Vincent E, Poffenberger M, Jones RG. The AMP-activated protein kinase (AMPK) and cancer: many faces of a metabolic regulator. Cancer Lett. 2015;356:165-70.
3. Jeon S, Hay N. The double-edged sword of AMPK signaling in cancer and its therapeutic implications. Arch Pharm Res. 2015;38:346-57.
4. Wang W, Guan K. AMP-activated protein kinase and cancer. Acta Physiol (Oxf). 2009;196:55-63.
5. Zadra G, Batista J, Loda M. Dissecting the dual role of AMPK in cancer: from experimental to human studies. Mol Cancer Res. 2015;13:1059-72.
6. Istvan ES, Deisenhofer J. Structural mechanism for statin inhibition of HMG-CoA reductase. Science 2001;292:1160-4.
7. Hebert PR, Gaziano JM, Chan KS, Hennekens CH. Cholesterol lowering with statin drugs, risk of stroke, and total mortality. An overview of randomized trials. JAMA 1997;278:313-21.
8. Greenwood J, Mason JC. Statins and the vascular endothelial inflammatory response. Trends Immunol. 2007;28:88-98.
9. Weis M, Heeschen C, Glassford AJ, Cooke JP. Statins have biphasic effects on angiogenesis. Circulation. 2002;105:739-45.
10. Sun W, Lee TS, Zhu M, Gu C, Wang Y, Zhu Y, et al. Statins activate AMP-activated protein kinase in vitro and in vivo. Circulation. 2006;114:2655-62.
11. Izumi Y, Shiota M, Kusakabe H, Hikita Y, Nakao T, Nakamura Y, et al. Pravastatin accelerates ischemia-induced angiogenesis through AMP-activated protein kinase. Hypertens Res. 2009;32:675-9.
12. Wang JC, Li XX, Sun X, Li GY, Sun JL, Ye YP, et al. Activation of AMPK by simvastatin inhibited breast tumor angiogenesis via impeding HIF-1α-induced pro-angiogenic factor. Cancer Sci. 2018;109:1627-37.
13. Kamel WA, Sugihara E, Nobusue H, Yamaguchi-Iwai S, Onishi N, Maki K, et al. Simvastatin-induced apoptosis in osteosarcoma cells: a key role of RhoA-AMPK/p38 MAPK signaling in antitumor activity. Mol Cancer Ther. 2017;16:182-92.
14. Wang ST, Ho HJ, Lin JT, Shieh JJ, Wu CY. Simvastatin-induced cell cycle arrest through inhibition of STAT3/SKP2 axis and activation of AMPK to promote p27 and p21 accumulation in hepatocellular

carcinoma cells. Cell Death Dis. 2017;8:e2626.

15. Strandberg TE, Pyörälä K, Cook TJ, Wilhelmsen L, Faergeman O, Thorgeirsson G, et al. Mortality and incidence of cancer during 10-year follow-up of the Scandinavian Simvastatin Survival Study (4S). Lancet. 2004;364:771-7.
16. Olzscha H, Sheikh S, La Thangue NB. Deacetylation of chromatin and gene expression regulation: a new target for epigenetic therapy. Crit Rev Oncog. 2015;20:1-17.
17. Bolden JE, Peart MJ, Johnstone RW. Anticancer activities of histone deacetylase inhibitors. Nat Rev Drug Discov. 2006;5:769-84.
18. Pinkerneil M, Hoffmann MJ, Deenen R, Köhrer K, Arent T, Schulz WA, et al. Inhibition of class I histone deacetylases 1 and 2 promotes urothelial carcinoma cell death by various mechanisms. Mol Cancer Ther. 2016;15:299-312.
19. Kaletsch A, Pinkerneil M, Hoffmann MJ, Jaguva Vasudevan AA, Wang C, Hansen FK, et al. Effects of novel HDAC inhibitors on urothelial carcinoma cells. Clin Epigenetics. 2018;10:100.
20. Giannopoulou AF, Velentzas AD, Konstantakou EG, Avgeris M, Katarachia SA, Papandreou NC, et al. Revisiting histone deacetylases in human tumorigenesis: the paradigm of urothelial bladder cancer. Int J Mol Sci. 2019;20:1291.
21. Furumai R, Matsuyama A, Kobashi N, Lee KH, Nishiyama M, Nakajima H, et al. FK228 (depsipeptide) as a natural prodrug that inhibits class I histone deacetylases. Cancer Res 2002;62:4916-21.
22. Greshock TJ, Johns DM, Noguchi Y, Williams RM. Improved total synthesis of the potent HDAC inhibitor FK228 (FR-901228). Org Lett. 2008;10:613-6.
23. Whittaker SJ, Demierre MF, Kim EJ, Rook AH, Lerner A, Duvic M, et al. Final results from a multicenter, international, pivotal study of romidepsin in refractory cutaneous T-cell lymphoma. J Clin Oncol. 2010;28:4485-91.
24. Niesvizky R, Ely S, Mark T, Aggarwal S, Gabrilove JL, Wright JJ, et al. Phase 2 trial of the histone deacetylase inhibitor romidepsin for the treatment of refractory multiple myeloma. Cancer. 2011;117:336-42.
25. Haigentz M Jr, Kim M, Sarta C, Lin J, Keresztes RS, Culliney B, et al. Phase II trial of the histone deacetylase inhibitor romidepsin in patients with recurrent/metastatic head and neck cancer. Oral Oncol. 2012;48:1281-8.
26. Amiri-Kordestani L, Luchenko V, Peer CJ, Ghafourian K, Reynolds J, Draper D, et al. Phase I trial of a new schedule of romidepsin in patients with advanced cancers. Clin Cancer Res. 2013;19:4499-507.
27. Zhang M, Galdieri L, Vancura A. The yeast AMPK homolog SNF1 regulates acetyl coenzyme A homeostasis and histone acetylation. Mol Cell Biol. 2013;33:4701-17.
28. Salminen A, Kauppinen A, Kaarniranta K. AMPK/Snf1signaling regulates histone acetylation: impact on gene expression and epigenetic functions. Cell Signal. 2016;28:887-95.
29. Okubo K, Isono M, Asano T, Sato A. Metformin augments panobinostat's anti-bladder cancer activity by activating AMP-activated protein kinase. Transl Oncol. 2019;12:669-82.

30. Okubo K, Isono M, Miyai K, Asano T, Sato A. Fluvastatin potentiates anticancer activity of vorinostat in renal cancer cells. Cancer Sci. 2020;111:112-26.
31. Berger J, Tanen M, Elbrecht A, Hermanowski-Vosatka A, Moller DE, Wright SD, et al. Peroxisome proliferator-activated receptor-gamma ligands inhibit adipocyte 11beta -hydroxysteroid dehydrogenase type 1 expression and activity. J Biol Chem. 2001;276:12629-35.
32. Berger J, Moller DE. The mechanisms of action of PPARs. Annu Rev Med. 2002;53:409-35.
33. Berger J, Wagner JA. Physiological and therapeutic roles of peroxisome proliferator-activated receptors. Diabetes Technol Ther. 2002;4:163-74.
34. Mansure JJ, Nassim R, Kassouf W. Peroxisome proliferator-activated receptor gamma in bladder cancer: a promising therapeutic target. Cancer Biol Ther. 2009;8:6-15.
35. Wang G, Cao R, Wang Y, Qian G, Dan HC, Jiang W, et al. Simvastatin induces cell cycle arrest and inhibits proliferation of bladder cancer cells via PPARγ signaling pathway. Sci Rep. 2016;6:35783.
36. Yousefnia S, Momenzadeh S, Seyed Forootan F, Ghaedi K, Nasr Esfahani MH. The influence of peroxisome proliferator-activated receptor γ (PPARγ) ligands on cancer cell tumorigenicity. Gene. 2018;649:14-22.
37. Workman P, Aboagye EO, Balkwill F, Balmain A, Bruder G, Chaplin DJ, et al. Guidelines for the welfare and use of animals in cancer research. Br J Cancer. 2010;102:1555-77.
38. Chou TC. Drug combination studies and their synergy quantification using the Chou-Talalay method. Cancer Res. 2010;70:440-6.
39. Srivastava N, Kollipara RK, Singh DK, Sudderth J, Hu Z, Nguyen H, et al. Inhibition of cancer cell proliferation by PPARγ is mediated by a metabolic switch that increases reactive oxygen species levels. Cell Metab. 2014;20:650-61.
40. Ram BM, Ramakrishna G. Endoplasmic reticulum vacuolation and unfolded protein response leading to paraptosis like cell death in cyclosporine A treated cancer cervix cells is mediated by cyclophilin B inhibition. Biochim Biophys Acta. 2014;1843:2497-512.
41. Wu J, Chen S, Liu H, Zhang Z, Ni Z, Chen J, et al. Tunicamycin specifically aggravates ER stress and overcomes chemoresistance in multidrug-resistant gastric cancer cells by inhibiting N-glycosylation. J Exp Clin Cancer Res. 2018;37:272.
42. Ashburn TT, Thor KB. Drug repositioning: identifying and developing new uses for existing drugs. Nat Rev Drug Discov. 2004;3:673-83.
43. Nowak-Sliwinska P, Scapozza L, Ruiz I Altaba A. Drug repurposing in oncology: Compounds, pathways, phenotypes and computational approaches for colorectal cancer. Biochim Biophys Acta Rev Cancer. 2019;1871:434-54.
44. Ciliberto G, Mancini R, Paggi MG. Drug repurposing against COVID-19: focus on anticancer agents. J Exp Clin Cancer Res. 2020;39:86.

45. Pedersen TR, Kjekshus J, Berg K, Olsson AG, Wilhelmsen L, Wedel H, et al. Cholesterol lowering and the use of healthcare resources. Results of the Scandinavian Simvastatin Survival Study. Circulation. 1996;93:1796-802.

46. Ridker PM, Pradhan A, MacFadyen JG, Libby P, Glynn RJ. Cardiovascular benefits and diabetes risks of statin therapy in primary prevention: an analysis from the JUPITER trial. Lancet. 2012;380:565-71.
47. Forrester JS, Libby P. The inflammation hypothesis and its potential relevance to statin therapy. Am J Cardiol. 2007;99:732-8.
48. Greenwood J, Mason JC. Statins and the vascular endothelial inflammatory response. Trends Immunol. 2007;28:88-98.
49. Zeiser R. Immune modulatory effects of statins. Immunology. 2018;154:69-75.
50. Chan KK, Oza AM, Siu LL. The statins as anticancer agents. Clin Cancer Res. 2003;9:10-9.
51. Demierre MF, Higgins PD, Gruber SB, Hawk E, Lippman SM. Statins and cancer prevention. Nat Rev Cancer. 2005;5:930-42.
52. Agarwal B, Bhendwal S, Halmos B, Moss SF, Ramey WG, Holt PR. Lovastatin augments apoptosis induced by chemotherapeutic agents in colon cancer cells. Clin Cancer Res. 1999;5:2223-9.
53. Wachtershauser A, Akoglu B, Stein J. HMG-CoA reductase inhibitor mevastatin enhances the growth inhibitory effect of butyrate in the colorectal carcinoma cell line Caco-2. Carcinogenesis. 2001;22:1061-7.
54. Lin Z, Zhang Z, Jiang X, Kou X, Bao Y, Liu H, et al. Mevastatin blockade of autolysosome maturation stimulates LBH589-induced cell death in triple-negative breast cancer cells. Oncotarget. 2017;8:17833-48.
55. Kou X, Yang Y, Jiang X, Liu H, Sun F, Wang X, et al. Vorinostat and simvastatin have synergistic effects on triple-negative breast cancer cells via abrogating Rab7 prenylation. Eur J Pharmacol. 2017;813:161-71.
56. Todd PA, Goa KL. Simvastatin. A review of its pharmacological properties and therapeutic potential in hypercholesterolaemia. Drugs. 1990;40:583-607.
57. Spampanato C, De Maria S, Sarnataro M, Giordano E, Zanfardino M, Baiano S, et al. Simvastatin inhibits cancer cell growth by inducing apoptosis correlated to activation of Bax and down-regulation of BCL-2 gene expression. Int J Oncol. 2012;40:935-41.
58. Lee J, Lee I, Han B, Park JO, Jang J, Park C, et al. Effect of simvastatin on cetuximab resistance in human colorectal cancer with KRAS mutations. J Natl Cancer Inst. 2011;103:674-88.
59. Lee Y, Lee KH, Lee GK, Lee SH, Lim KY, Joo J, et al. Randomized phase II study of afatinib plus simvastatin versus afatinib alone in previously treated patients with advanced nonadenocarcinomatous non-small cell lung cancer. Cancer Res Treat. 2017;49:1001-11.

60. El-Hamamsy M, Elwakil H, Saad AS, Shawki MA. A randomized controlled open-label pilot study of simvastatin addition to whole-brain radiation therapy in patients with brain metastases. Oncol Res. 2016;24:521-28.
61. Lim SH, Kim TW, Hong YS, Han SW, Lee KH, Kang HJ, et al. A randomised, double-blind, placebo-controlled multi-centre phase III trial of XELIRI/FOLFIRI plus simvastatin for patients with metastatic colorectal cancer. Br J Cancer. 2015;113:1421-6.
62. Kim ST, Kang JH, Lee J, Park SH, Park JO, Park YS, et al. Simvastatin plus capecitabine-cisplatin versus placebo plus capecitabine-cisplatin in patients with previously untreated advanced gastric cancer: a double-blind randomised phase 3 study. Eur J Cancer. 2014;50:2822-30.
63. Hong JY, Nam EM, Lee J, Park JO, Lee SC, Song SY, et al. Randomized double-blinded, placebo-controlled phase II trial of simvastatin and gemcitabine in advanced pancreatic cancer patients. Cancer Chemother Pharmacol. 2014;73:125-30.
64. Han JY, Lee SH, Yoo NJ, Hyung LS, Moon YJ, Yun T, et al. A randomized phase II study of gefitinib plus simvastatin versus gefitinib alone in previously treated patients with advanced non-small cell lung cancer. Clin Cancer Res. 2011;17:1553-60.
65. Tennant DA, Durán RV, Gottlieb E. Targeting metabolic transformation for cancer therapy. Nat Rev Cancer. 2010;10:267-77.
66. Cantor JR, Sabatini DM. Cancer cell metabolism: one hallmark, many faces. Cancer Discov. 2012;2:881-98.
67. Grunstein M. Histone acetylation in chromatin structure and transcription. Nature. 1997;389:349-52.
68. Marks P, Rifkind RA, Richon VM, Breslow R, Miller T, Kelly WK. Histone deacetylase and cancer: causes and therapies. Nat Rev Cancer. 2001;1:194-202.
69. Gallinari P, Di Marco S, Jones P, Pallaoro M, Steinkühler C. HDACs, histone deacetylation and gene transcription: from molecular biology to cancer therapeutics. Cell Res. 2007;17:195-211.
70. Bali P, Pranpat M, Bradner J, Balasis M, Fiskus W, Guo F, et al. Inhibition of histone deacetylase 6 acetylates and disrupts the chaperone function of heat shock protein 90: a novel basis for antileukemia activity of histone deacetylase inhibitors. J Biol Chem. 2005;280:26729-34.
71. Fiskus W, Ren Y, Mohapatra A, Bali P, Mandawat A, Rao R, et al. Hydroxamic acid analogue histone deacetylase inhibitors attenuate estrogen receptor-alpha levels and transcriptional activity: a result of hyperacetylation and inhibition of chaperone function of heat shock protein 90. Clin Cancer Res. 2007;13:4882-90.
72. Baumeister P, Dong D, Fu Y, Lee AS. Transcriptional induction of GRP78/BiP by histone deacetylase inhibitors and resistance to histone deacetylase inhibitor-induced apoptosis. Mol Cancer Ther. 2009;8:1086-94.
73. Sato A, Asano T, Okubo K, Isono M, Asano T. Nelfinavir and ritonavir kill bladder cancer cells synergistically by inducing endoplasmic reticulum stress. Oncol Res. 2018;26:323-32.
74. Okubo K, Isono M, Asano T, Sato A. Panobinostat and nelfinavir inhibit renal cancer growth by inducing endoplasmic reticulum stress. Anticancer Res. 2018;38:5615-26.

75. Walter P, Ron D. The unfolded protein response: from stress pathway to homeostatic regulation. Science. 2011;334:1081-6.
76. Liu Y, Ye Y. Proteostasis regulation at the endoplasmic reticulum: a new perturbation site for targeted cancer therapy. Cell Res. 2011;21:867-83.
77. Tabas I, Ron D. Integrating the mechanisms of apoptosis induced by endoplasmic reticulum stress. Nat Cell Biol. 2011;13:184-90.
78. Mimnaugh EG, Xu W, Vos M, Yuan X, Isaacs JS, Bisht KS, et al. Simultaneous inhibition of hsp 90 and the proteasome promotes protein ubiquitination, causes endoplasmic reticulum-derived cytosolic vacuolization, and enhances antitumor activity. Mol Cancer Ther. 2004;3:551-66.
79. Okubo K, Sato A, Isono M, Asano T, Asano T. Nelfinavir induces endoplasmic reticulum stress and sensitizes renal cancer cells to TRAIL. Anticancer Res. 2018;38:4505-14.
80. Sato A, Asano T, Okubo K, Isono M, Asano T. Ritonavir and ixazomib kill bladder cancer cells by causing ubiquitinated protein accumulation. Cancer Sci. 2017;108:1194-202.
81. Berger JP, Akiyama TE, Meinke PT. PPARs: Therapeutic targets for metabolic disease. Trends Pharmacol Sci. 2005;26:244-51.
82. Mueller E, Smith M, Sarraf P, Kroll T, Aiyer A, Kaufman DS, et al. Effects of ligand activation of peroxisome proliferator-activated receptor gamma in human prostate cancer. Proc Natl Acad Sci U S A. 2000;97:10990-5.
83. Grommes C, Landreth GE, Heneka MT. Antineoplastic effects of peroxisome proliferator-activated receptor gamma agonists. Lancet Oncol. 2004;5:419-29.
84. Kubota T, Koshizuka K, Williamson EA, Asou H, Said JW, Holden S, et al. Ligand for peroxisome proliferator-activated receptor gamma (troglitazone) has potent antitumor effect against human prostate cancer both in vitro and in vivo. Cancer Res. 1998;58:3344-52.
85. Burstein HJ, Demetri GD, Mueller E, Sarraf P, Spiegelman BM, Winer EP. Use of the peroxisome proliferator-activated receptor (PPAR) gamma ligand troglitazone as treatment for refractory breast cancer: a phase II study. Breast Cancer Res Treat. 2003;79:391-7.
86. Kulke MH, Demetri GD, Sharpless NE, Ryan DP, Shivdasani R, Clark JS, et al. A phase II study of troglitazone, an activator of the PPARgamma receptor, in patients with chemotherapy-resistant metastatic colorectal cancer. Cancer J. 2002;8:395-9.
87. Hau P, Kunz-Schughart L, Bogdahn U, Baumgart U, Hirschmann B, Weimann E, et al. Low-dose chemotherapy in combination with COX-2 inhibitors and PPAR-gamma agonists in recurrent high-grade gliomas - a phase II study. Oncology. 2007;73:21-5.
88. Smith MR, Manola J, Kaufman DS, George D, Oh WK, Mueller E, et al. Rosiglitazone versus placebo for men with prostate carcinoma and a rising serum prostate-specific antigen level after radical prostatectomy and/or radiation therapy. Cancer. 2004;101:1569-74.
89. Paltoo D, Woodson K, Taylor P, Albanes D, Virtamo J, Tangrea J. Pro12Ala polymorphism in the peroxisome proliferator-activated receptor-gamma (PPAR-gamma) gene and risk of prostate cancer among men in a large cancer prevention study. Cancer Lett. 2003;191:67-74.

90. Tepmongkol S, Keelawat S, Honsawek S, Ruangvejvorachai P. Rosiglitazone effect on radioiodine uptake in thyroid carcinoma patients with high thyroglobulin but negative total body scan: a correlation with the expression of peroxisome proliferator-activated receptor-gamma. Thyroid. 2008;18:697-704.
91. Aouali N, Palissot V, El-Khoury V, Moussay E, Janji B, Pierson S, et al. Peroxisome proliferator-activated receptor gamma agonists potentiate the cytotoxic effect of valproic acid in multiple myeloma cells. Br J Haematol. 2009;147:662-71.
92. Davies GF, Ross AR, Arnason TG, Juurlink BH, Harkness TA. Troglitazone inhibits histone deacetylase activity in breast cancer cells. Cancer Lett. 2010;288:236-50.
93. Aouali N, Broukou A, Bosseler M, Keunen O, Schlesser V, Janji B, et al. Epigenetic activity of peroxisome proliferator-activated receptor gamma agonists increases the anticancer effect of histone deacetylase inhibitors on multiple myeloma cells. PLoS One. 2015;10:e0130339.

Tables

Table 1: Mean inhibitory concentrations (IC50) of various histone deacetylase (HDAC) inhibitors in bladder cancer cells

	HDAC inhibitors (μM)				
	Romidepsin	Panobinostat	Belinostat	Vorinostat	Entinostat
UMUC-3	0.01215	0.16008	1.26107	6.76897	17.4520
T-24	0.02916	0.06688	8.62434	11.6635	110.027

After bladder cancer cells were treated for 48 hours with various HDAC inhibitors, cell viability was measured using CCK-8 assay and IC50 values were calculated.

Table 2: Combination indexes (CIs) for the combination of 2.5–5 μM simvastatin and 5–20 nM romidepsin in bladder cancer cells

	Romidepsin (nM)		
Simvastatin (μM)	5	10	20
UMUC-3			
2.5	0.599	0.288	0.090
5	0.247	0.080	0.020
T-24			
2.5	0.465	0.488	0.559
5	0.603	0.397	0.192
J-82			
2.5	0.806	0.657	0.855
5	0.576	0.562	0.548
MBT-2			
2.5	0.862	0.234	0.170
5	0.803	0.242	0.117

CI < 1 indicates synergy.

Table 3: Combination indexes (CIs) for the combination of 50–100 μM rosiglitazone and 5–20 nM romidepsin in bladder cancer cells

	Romidepsin (nM)		
Rosiglitazone (μM)	5	10	20
UMUC-3			
50	0.314	0.311	0.256
100	0.223	0.224	0.189
T-24			
50	0.705	0.660	0.633
100	0.857	0.793	0.779

CI < 1 indicates synergy.

Table 4 Clinical trials using simvastatin in patients with various types of cancer

Study design	Cancer type	Combined drugs or radiation	Disease stage	Number of patients Simvastatin/Control	Results		References
					Median OS (months) Simvastatin/Control	P value	
Phase II	Non-ADC NSCLC	Afatinib	Advanced (stage IIIB/IV)	36/32	10.0/7.0	0.93	Lee Y, et al.
Phase III	Any	Radiation	Brain metastases	25/25	3.4/3.0	0.88	El-Hamamsy M, et al.
Phase III	Colorectal cancer	XELIRI or FOLFIRI	Metastatic (stage IV)	134/135	15.3/19.2	0.83	Lim SH, et al.
Phase III	Gastric cancer	Capecitabine + cisplatin	Metastatic (stage IV)	120/124	11.6/11.5	0.82	Kim ST, et al.
Phase II	Pancreatic cancer	Gemcitabine	Locally advanced or metastatic	58/56	6.6/8.9	0.74	Hong JY, et al.
Phase II	NSCLC	Gefitinib	Locally advanced or metastatic (stage IIIB-IV)	52/54	13.6/12	0.49	Han JY, et al.

ADC, adenocarcinomatous; FOLFIRI, 5-FU + leucovorin + irinotecan; NSCLC, non-small cell lung cancer; OS, overall survival; XELIRI, capecitabine + irinotecan.

Figures

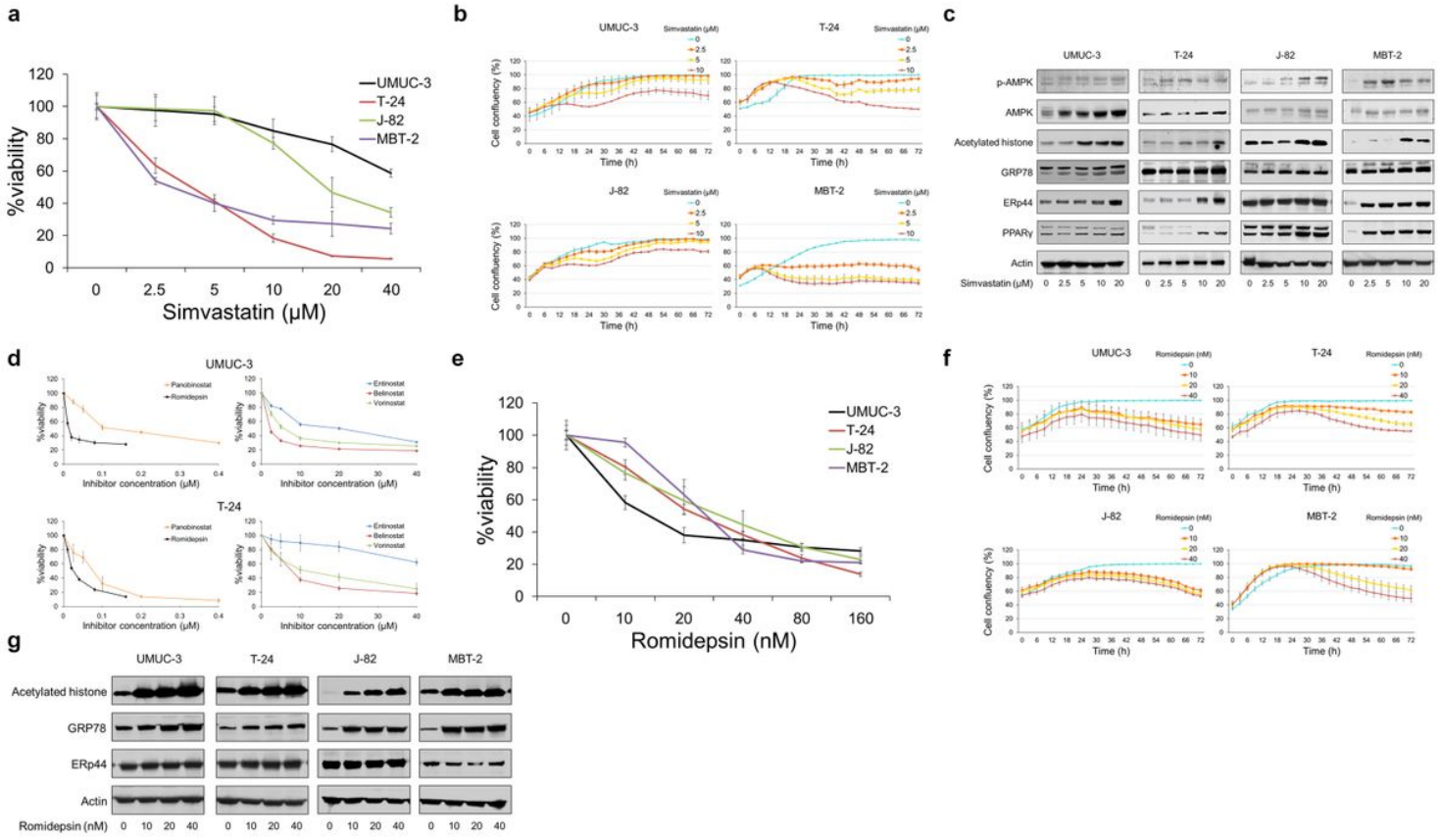

Figure 1

Anticancer activity of simvastatin and romidepsin in bladder cancer cells. a Cells were treated for 48 hours with 2.5–40 μM simvastatin and cell viability was measured using CCK-8 assay. Mean ± SD, n = 6. b Cells were given 2.5–10 μM simvastatin and confluence measurements were performed at 3-hour intervals over 3 days. Mean ± SD, n = 6. c Western blotting for AMP-activated protein kinase (AMPK), acetylated histone, glucose-regulated protein (GRP) 78, endoplasmic reticulum resident protein (ERp) 44, and peroxisome proliferator-activated receptor (PPAR) γ. Cells were treated for 48 hours with 2.5–20 μM simvastatin. Actin was used for the loading control. Representative blots are shown. d Cells were treated for 48 hours with different concentrations of various histone deacetylase (HDAC) inhibitors, and cell viability was measured using CCK-8 assay. Mean ± SD, n = 6. e Cells were treated for 48 hours with 10–160 nM romidepsin and cell viability was measured using CCK-8 assay. Mean ± SD, n = 6. f Cells were given 10–40 nM romidepsin and confluence measurements were performed at 3-hour intervals over 3 days. Mean ± SD, n = 6. g Western blotting for acetylated histone, GRP78, and ERp44. Cells were treated for 48 hours with 10–40 nM romidepsin. Actin was used for the loading control. Representative blots are shown.

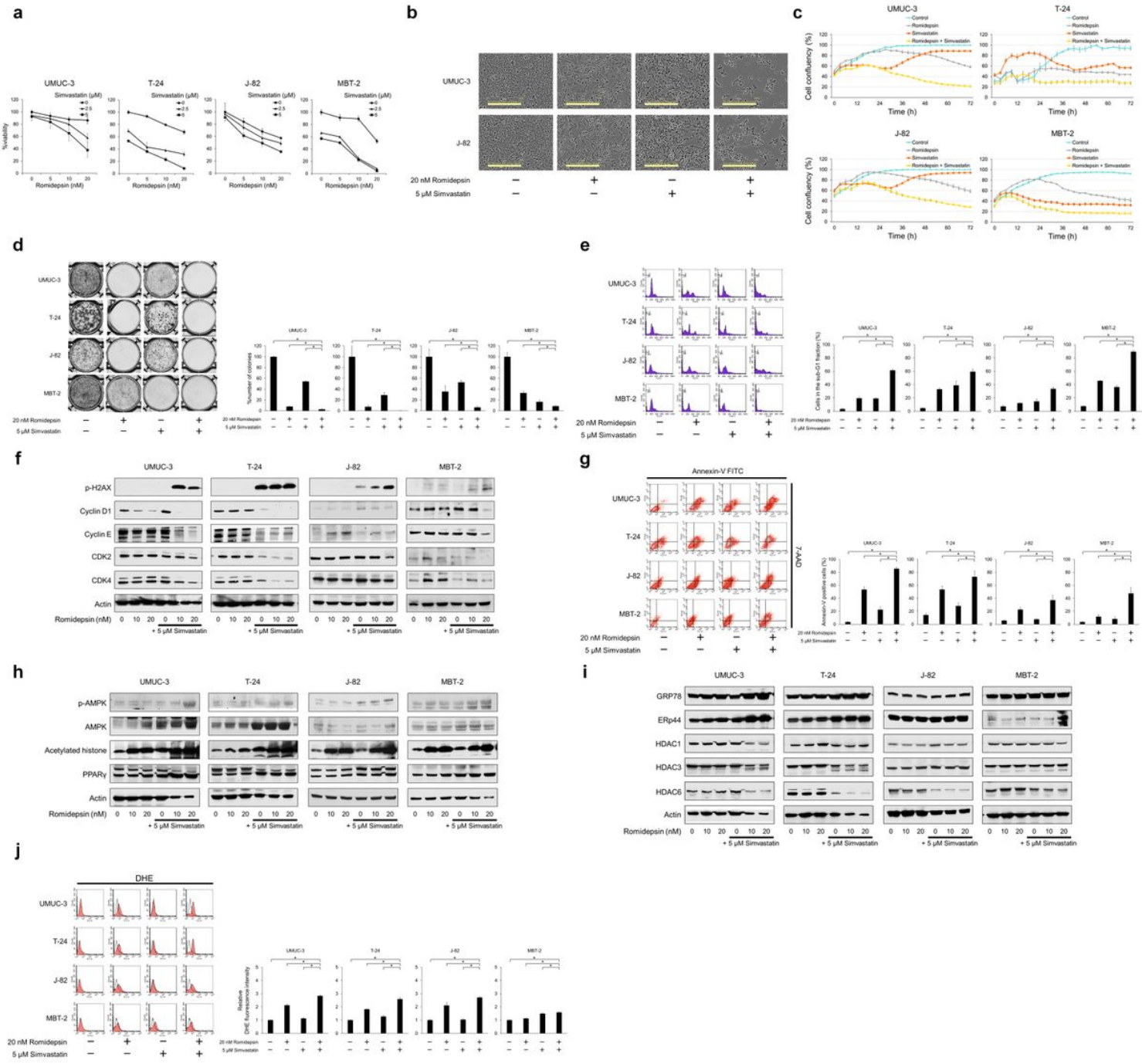

Figure 2

Anticancer activity of the simvastatin-romidepsin combination in bladder cancer cells. a Cells were treated for 48 hours with 2.5–5 μM simvastatin and/or 5–20 nM romidepsin and cell viability was measured using CCK-8 assay. Bars represent mean ± SD, n = 6. b Photomicrographs showing morphological changes of the cells after 48-hour treatment with 5 μM simvastatin and/or 20 nM romidepsin. Scale bar = 300 μm. c Cells were given 5 μM simvastatin and/or 20 nM romidepsin and confluence measurements were performed at 3-hour intervals over 3 days. Mean ± SD, n = 6. d Clonogenic assay. 200–300 cells were treated for 48 hours with 5 μM simvastatin and/or 20 nM romidepsin. The cells were then given fresh media and incubated for 1–2 weeks. Bar graphs show the

%number of colonies relative to the untreated control. Mean ± SD, n = 3. *p = 0.0495. e Cells were treated for 48 hours with 5 μM simvastatin and/or 20 nM romidepsin. Changes in the cell cycle were evaluated using flow cytometry. 10,000 cells were counted. Bar graphs show the percentages of the cells in the sub-G1 fraction. Data are expressed as mean ± SD from three independent experiments. *p = 0.0495. f Western blotting for phosphorylated histone H2AX (p-H2AX), cyclin D1, cyclin E, cyclin-dependent kinase (CDK) 2, and CDK4. Cells were treated with 5 μM simvastatin and/or 10–20 nM romidepsin for 48 hours. Actin was used for the loading control. Representative blots are shown. g Cells were treated for 48 hours with 5 μM simvastatin and/or 20 nM romidepsin. Apoptotic cells were detected by annexin-V assay using flow cytometry. 10,000 cells were counted. Bar graphs show the percentages of apoptotic cells. Data are expressed as mean ± SD from three independent experiments. FITC, fluorescein isothiocyanate; 7-AAD, 7-amino-actinomycin D. *p = 0.0495. h Western blotting for AMP-activated protein kinase (AMPK), acetylated histone, and peroxisome proliferator-activated receptor (PPAR) γ. Cells were treated with 5 μM simvastatin and/or 10–20 nM romidepsin for 48 hours. Actin was used for the loading control. Representative blots are shown. i Western blotting for glucose-regulated protein (GRP) 78, endoplasmic reticulum resident protein (ERp) 44, histone deacetylase (HDAC) 1, HDAC3, and HDAC6. Cells were treated with 5 μM simvastatin and/or 10–20 nM romidepsin for 48 hours. Actin was used for the loading control. Representative blots are shown. j Cells were treated with 5 μM simvastatin and/or 20 nM romidepsin for 48 hours and reactive oxygen species production was measured by dihydroethidium (DHE) staining using flow cytometry. 10,000 cells were counted. Bar graphs show the relative DHE fluorescence intensity. Data are expressed as mean ± SD from three independent experiments. *p = 0.0495.

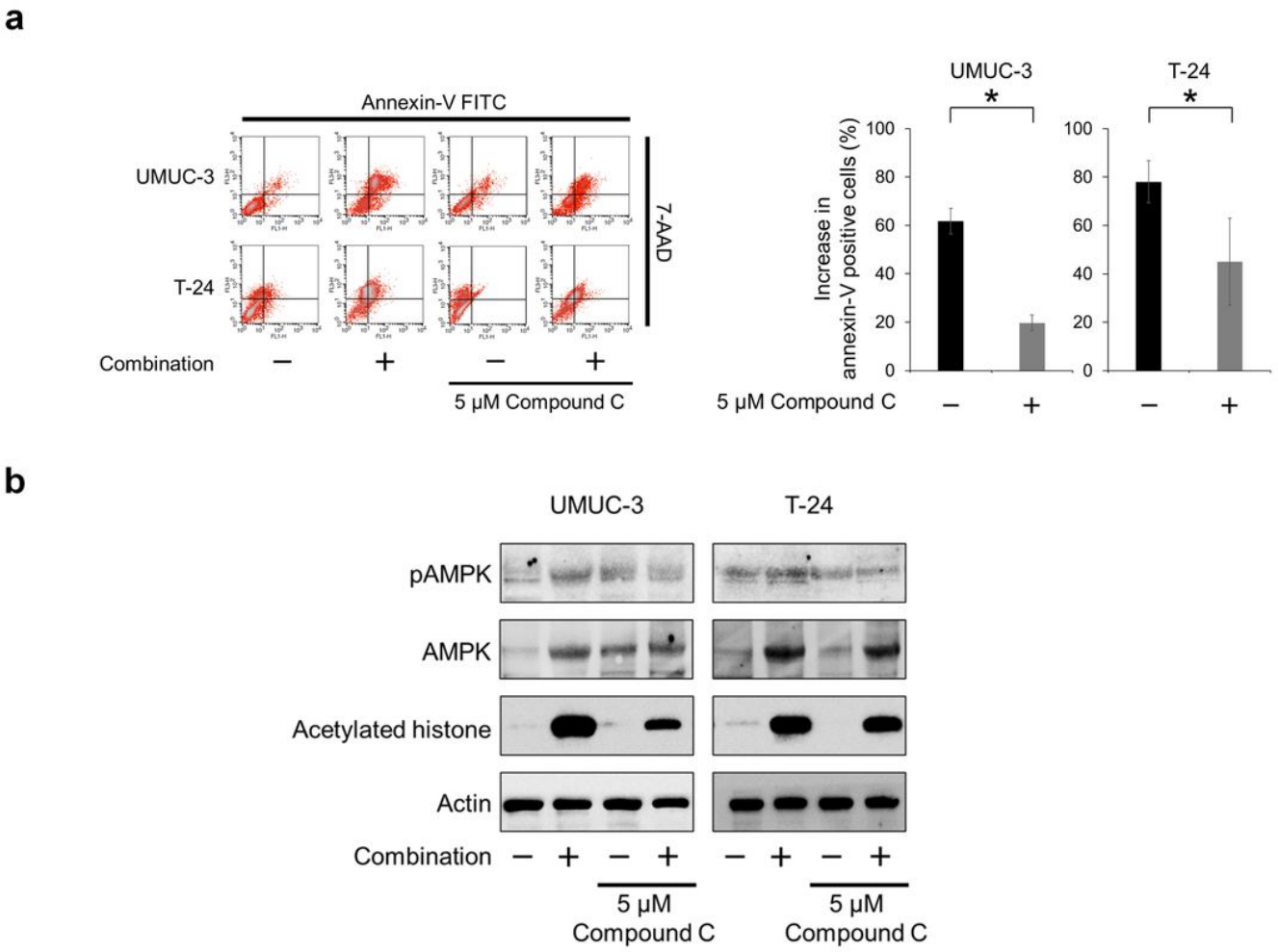

Figure 3

AMP-activated protein kinase (AMPK) activation was responsible for the enhanced histone acetylation and cytotoxicity caused by the simvastatin-romidepsin combination. a Cells were treated for 48 hours with 5 μM simvastatin and 20 nM romidepsin with or without 5 μM compound C. Apoptotic cells were detected by annexin-V assay using flow cytometry. 10,000 cells were counted. Bar graphs show the increase in annexin-V positive cells. Data are expressed as mean ± SD from three independent experiments. FITC, fluorescein isothiocyanate; 7-AAD, 7-amino-actinomycin D. *p = 0.0495. b Western blotting for AMPK and acetylated histone. Cells were treated for 48 hours with 5 μM simvastatin and 20 nM romidepsin with or without 5 μM compound C. Actin was used for the loading control. Representative blots are shown.

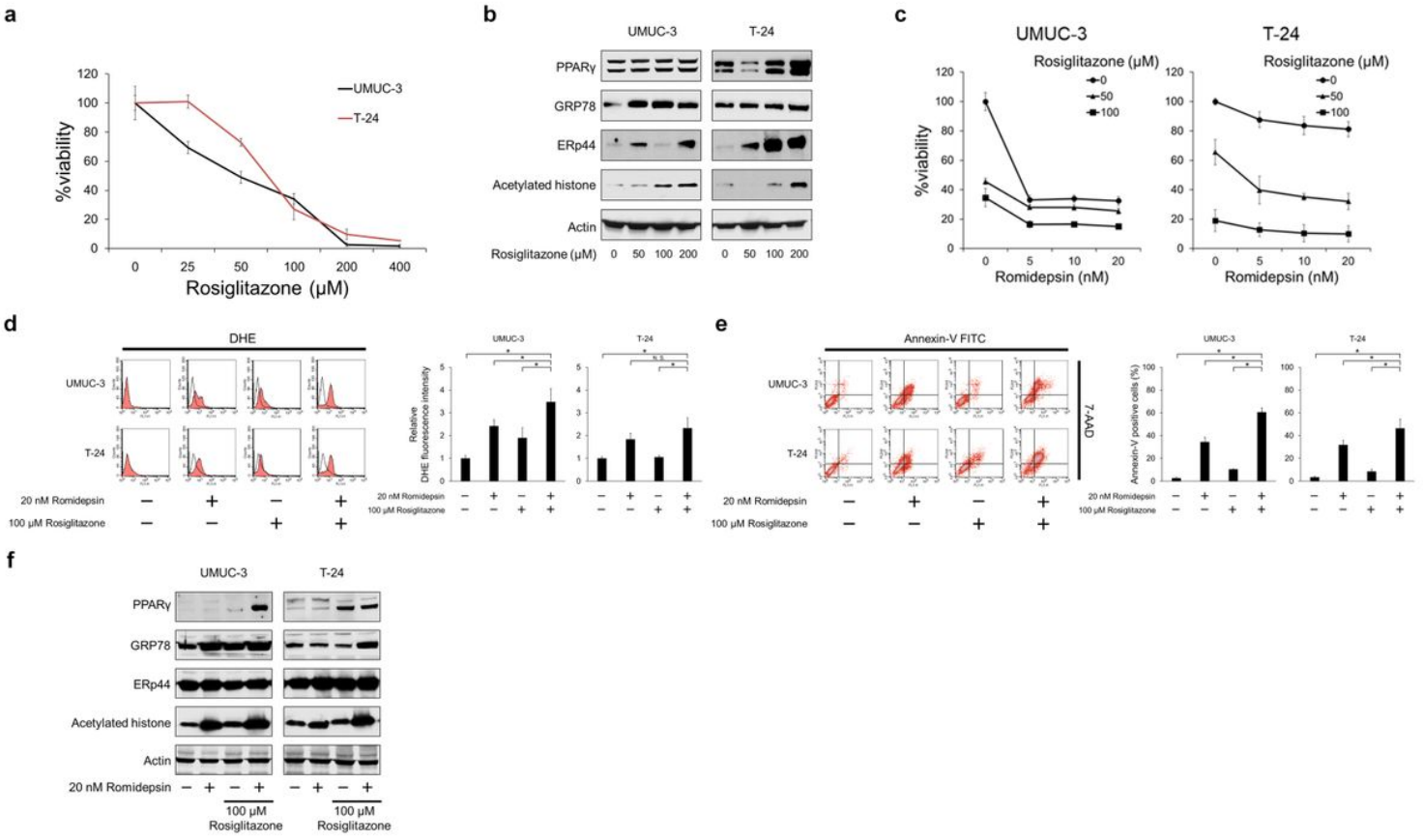

Figure 4

Peroxisome proliferator-activated receptor (PPAR) γ activation played a pivotal role in killing bladder cancer cells. a Cells were treated for 48 hours with 25–400 μM rosiglitazone and cell viability was measured using CCK-8 assay. Mean ± SD, n = 6. b Western blotting for PPARγ, glucose-regulated protein (GRP) 78, endoplasmic reticulum resident protein (ERp) 44, and acetylated histone. Cells were treated for 48 hours with 50–200 μM rosiglitazone. Actin was used for the loading control. Representative blots are shown. c Cells were treated for 48 hours with 50–100 μM rosiglitazone and/or 5–20 nM romidepsin and cell viability was measured using CCK-8 assay. Bars represent mean ± SD, n = 6. d Cells were treated for 48 hours with 100 μM rosiglitazone and/or 20 nM romidepsin and reactive oxygen species production was measured by dihydroethidium (DHE) staining using flow cytometry. 10,000 cells were counted. Bar graphs show the relative DHE fluorescence intensity. Data are expressed as mean ± SD from three independent experiments. *p = 0.0495; N. S., not significant. e Cells were treated for 48 hours with 100 μM rosiglitazone and/or 20 nM romidepsin. Apoptotic cells were detected by annexin-V assay using flow cytometry. 10,000 cells were counted. Bar graphs show the percentages of apoptotic cells. Data are expressed as mean ± SD from three independent experiments. FITC, fluorescein isothiocyanate; 7-AAD, 7-amino-actinomycin D. *p = 0.0495. f Western blotting for PPARγ, GRP78, ERp44, and acetylated histone. Cells were treated for 48 hours with 100 μM rosiglitazone and/or 20 nM romidepsin. Actin was used for the loading control. Representative blots are shown.

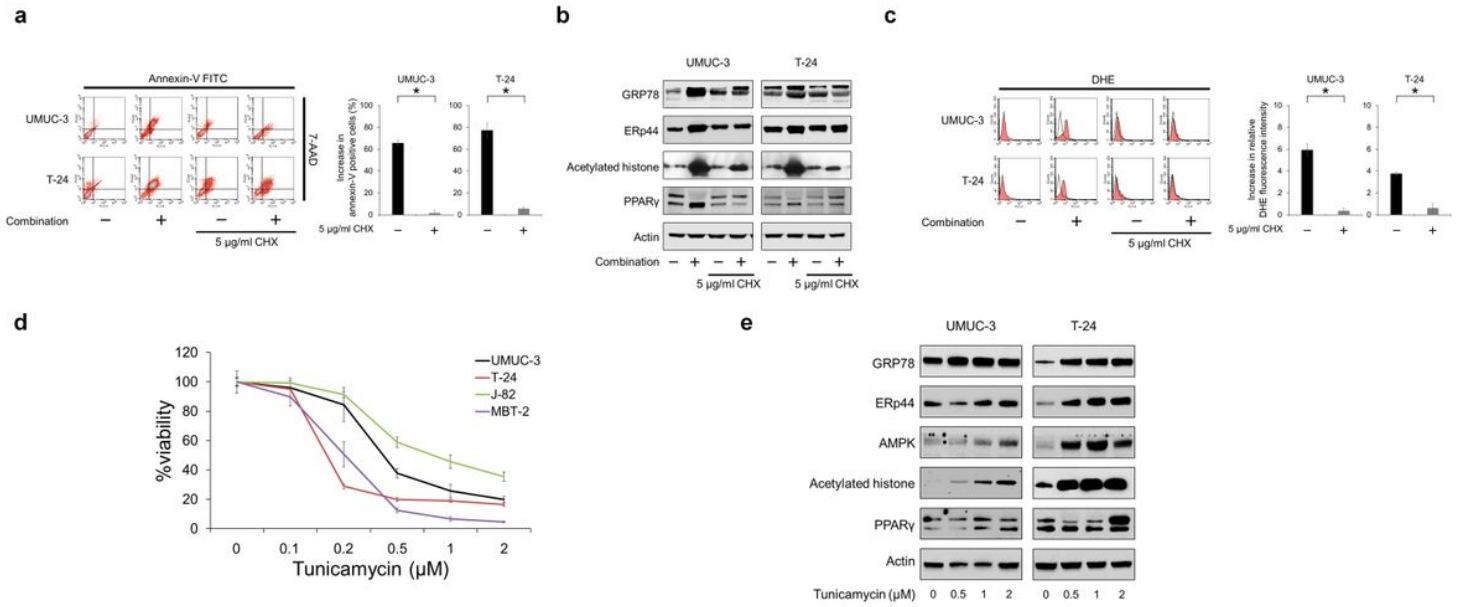

Figure 5

Endoplasmic reticulum stress induction is also an important mechanism of the combination's action. a Cells were treated for 48 hours with 5 μM simvastatin and 20 nM romidepsin with or without 5 μg/ml cycloheximide (CHX). Apoptotic cells were detected by annexin-V assay using flow cytometry. 10,000 cells were counted. Bar graphs show the increase in annexin-V positive cells. Data are expressed as mean ± SD from three independent experiments. FITC, fluorescein isothiocyanate; 7-AAD, 7-amino-actinomycin D. *p = 0.0495. b Western blotting for glucose-regulated protein (GRP) 78, endoplasmic reticulum resident protein (ERp) 44, acetylated histone, and peroxisome proliferator-activated receptor (PPAR) γ. Cells were treated for 48 hours with 5 μM simvastatin and 20 nM romidepsin with or without 5 μg/ml CHX. Actin was used for the loading control. Representative blots are shown. c Cells were treated for 48 hours with 5 μM simvastatin and 20 nM romidepsin with or without 5 μg/ml CHX and reactive oxygen species production was measured by dihydroethidium (DHE) staining using flow cytometry. 10,000 cells were counted. Bar graphs show the increase in relative DHE fluorescence intensity. Data are expressed as mean ± SD from three independent experiments. *p = 0.0495. d Cells were treated for 48 hours with 0.1–2 μM tunicamycin and cell viability was measured using CCK-8 assay. Mean ± SD, n = 6. e Western blotting for GRP78, ERp44, AMP-activated protein kinase (AMPK), acetylated histone, and PPARγ. Cells were treated for 48 hours with 0.5–2 μM tunicamycin. Actin was used for the loading control. Representative blots are shown.

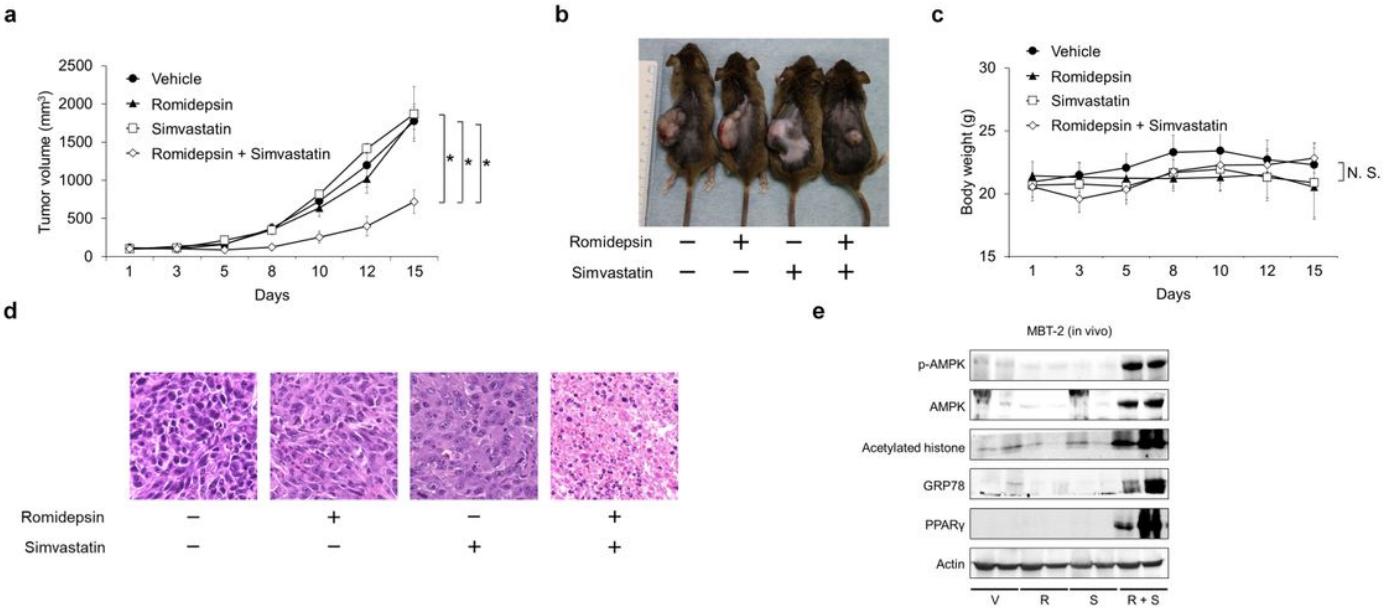

Figure 6

The simvastatin-romidepsin combination inhibited bladder cancer growth in vivo. a A murine allograft model was established using MBT-2 cells. The vehicle group received intraperitoneal injections of dimethyl sulfoxide (DMSO) and the treatment groups received 15 mg/kg simvastatin or 0.5 mg/kg romidepsin or both. The injections of romidepsin were given twice per week and the injections of DMSO and simvastatin were given once a day for 15 days (5 days on, 2 days off). Mean ± SE, n = 5. *p = 0.0079 at day 15. b A photograph of the mice after 15-day treatment. c Changes in the body weight. Mean ± SD, n = 5. Note that there is no significant difference in the body weight among each group at day 15. N. S., not significant. d Hematoxylin eosin (HE) staining of the tumors. After 15 days of treatment, the animals were euthanized and the subcutaneous tumors were harvested and evaluated by microscopy using HE staining. e Western blotting for AMP-activated protein kinase (AMPK), acetylated histone, glucose-regulated protein (GRP) 78, and peroxisome proliferator-activated receptor (PPAR) γ. After 15 days of treatment, the animals were euthanized and the subcutaneous tumors were harvested, lysed, and subjected to western blotting. Actin was used for the loading control. Representative blots are shown. V, vehicle-treated mice; R, romidepsin-treated mice; S, simvastatin-treated mice; R + S, combination-treated mice.

Supplementary Files

This is a list of supplementary files associated with this preprint. Click to download.

- Fig.S4rev.tif
- Fig.S4rev.tif
- Fig.S3rev.tif

- Fig.S3rev.tif
- Videoimages1.mp4
- Videoimages1.mp4
- Fig.S2rev.tif
- Fig.S2rev.tif
- Fig.S1.tif
- Fig.S1.tif